

600457

D1-82-0333

**BOEING** SCIENTIFIC  
RESEARCH  
LABORATORIES

25-p  
#0.75

Thermal Conductivity  
of Copper-Nickel Alloys at 4.2°K

DDC  
APR 1 1964  
TISIA E

Joachim C. Erdmann

James A. Jahoda

Solid State Physics Laboratory

April, 1964

D1-82-0333

THERMAL CONDUCTIVITY OF COPPER-NICKEL ALLOYS AT 4.2°K

by

Joachim C. Erdmann

and

James A. Jahoda

April, 1964

Boeing Scientific Research Laboratories

Seattle, Washington

## ABSTRACT

The lattice thermal conductivity  $\kappa_l$  of the complete Cu-Ni alloy series at 4.2 K has been derived from the measurement of the total thermal conductivity and the electrical residual resistivity of annealed specimens. It is found that  $\kappa_l$  decreases in the copper-rich alloys with increasing content of nickel. For most of the composition range, however,  $\kappa_l$  is proportional to the electrical residual resistivity. Thus, a minimum of  $\kappa_l$  vs. composition is observed at Cu 92 - Ni 08, and also a maximum at appr. Cu 55 - Ni 45. The result is consistent with current theories of Klemens and Pippard. For the most nickel-rich alloy (Cu 02 - Ni 98) indications of additional phonon scattering processes, perhaps by spin-disorder, are found. The influence of plastic deformation  $\kappa_l$  has been measured and is briefly discussed.

## I. Introduction

The lattice thermal conductivity of alloys has been investigated by many authors. The theoretical work of special interest for our purpose is listed as Refs. (1) to (12). Some of the experimental investigations (20)-(22) were carried out with annealed dilute alloys having low electrical resistivity, particularly alloys based on copper and silver. In those cases it was found that, at helium temperatures, the Wiedemann-Franz law holds well and also that the lattice conductivity varies proportional to the square of the absolute temperature, indicating scattering of phonons by electrons in substantial agreement with theories of Sommerfeld and Bethe,<sup>(1)</sup> and Makison.<sup>(2)</sup> Chari<sup>(24)</sup> found a maximum in the lattice conductivity of dilute silver-manganese alloys at 4°K and a  $T^3$  dependence below that temperature. He attributed this deviation from the ordinary behavior to scattering of phonons by magnetic domain walls.

In other investigations,<sup>(13)</sup> to (19) the effect of plastic deformation on the lattice conductivity has been studied. The additional thermal resistance due to dislocations was found to depend on the temperature as  $T^{-2}$  so that electron scattering and dislocation scattering of phonons cannot be separated merely on the basis of the temperature dependence. For a time, this methodical disadvantage led to uncertainties about the possible influence of dislocations on the composition dependence of the

lattice conductivity in dilute alloys. Observations of Kemp and Klemens<sup>(18)</sup> showed that the lattice conductivity in dilute alloys decreases with solute content, and it was concluded that dislocation locking, increasing with the number of solute atoms, is responsible for these observations. Later work by Tainsh and White,<sup>(21)</sup> Klemens, White and Tainsh,<sup>(22)</sup> Lindenfeld and Pennebaker<sup>(26)</sup> led to a different interpretation by Klemens et al.<sup>(22)</sup> who assumed that the inelastic scattering of electrons by thermally vibrating solute atoms, investigated by Koshino,<sup>(27)</sup> lowers the lattice conductivity.

In alloys with high electrical resistivity, it was found by Zimmerman<sup>(25)</sup> and Lindenfeld and Pennebaker<sup>(26)</sup> that a term proportional to the temperature and the electrical resistivity arises in the expression for the lattice conductivity in addition to the quadratic term. The effect had been predicted by Pippard,<sup>(28)</sup> and in fact the investigators of Refs. (25) and (26) were able to interpret their results in terms of the Pippard theory. The experiments were done using dilute silver-antimony and dilute copper alloys containing a few percent germanium, aluminum, gallium, or indium, respectively.

In this work we report about the thermal conductivity of the complete Cu-Ni series at 4.2°K. The results show the simultaneous presence of the composition effect of the type suggested by Klemens et al.<sup>(22)</sup> and of the high-resistance effect predicted by Pippard.<sup>(28)</sup> It is further shown that in annealed

Alloy No	Composition (Weight Percent)	Resistivity [ $\mu\text{ohms cm}$ ] at 4.2°K
868	1.96 Ni, Bal. Cu	2.17
664	4.74 Ni, 0.043 Al, <0.1 Mn, Mg, Fe, Bal. Cu.	7.04
666	9.3 Ni, 0.025 Al, Bal. Cu	10.94
667	27.96 Ni, 0.023 Al, <1.0 Fe, Mg, Bal. Cu	32.3
Ko	$\approx$ 40.0 Ni, Bal. Cu, Impurities unknown	42.3
669	64.87 Ni, 0.051 Al, 0.013 C, <0.01 Fe, Bal. Cu	27.8
670	84.7 Ni, 0.054 Al, 0.02C, <0.1 Fe, Mn, Bal. Cu	10.64
131	2.03 Cu, Bal. Ni	1.65

TABLE I. Composition and residual resistivity of the investigated Cu-Ni alloys.

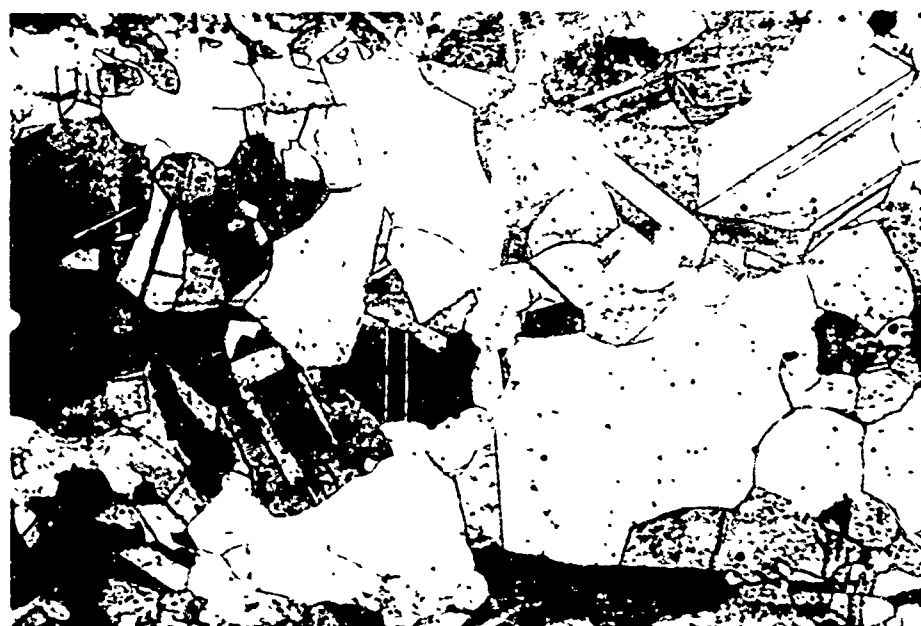


Fig. 1. Micrograph of alloy 664 ( $\approx$ 5% Ni).

nickel-rich alloys the lattice conductivity cannot be limited merely by electron-phonon processes. The influence of plastic deformation also is discussed.

## II. Experiments

### A. Sample Preparation.

Poly crystalline Cu-Ni alloys in the form of wires, together with their chemical analysis and spectrographic surveys were provided by the courtesy of the International Nickel Company, Inc. The vacuum cast ingots were hammer forged, hot rolled to 18.5 mm diameter and rough turned. The rough turned bars were cold rolled to 6 mm diameter and drawn to 1.5 mm diameter wire. Intermediate annealing was performed at  $930^{\circ}\text{C}$  when necessary. The wires were afterwards cut into pieces of 130 mm lengths, annealed in an argon atmosphere for 24 hours at  $1000^{\circ}\text{C}$ , and slowly cooled in the furnace over a period of 6 hours. They were then electropolished, having final diameters of 1.35 to 1.45 mm.

The reference numbers of the alloys, together with the composition and residual resistivity, are listed in Table I.

A typical micrograph of the etched surface of an alloy specimen after the final heat treatment is shown in Fig. 1. The grain size has a value between 50 and 250  $\mu$ .

For the experiments the wires were finally cut to a length of 125 mm. Each of the two ends of each wire was put through the axial hole drilled through a brass cylinder of 7.5 mm

diameter and 12 mm length, and brazed to the brass cylinder with a small flame. "Easy Flow 45" solder having a melting point of 620°C was used. To the center of the remaining free piece of wire (length 100 mm) and to a point 35 mm off the center, small soft copper clamps of approximately 0.75 mm thickness were soldered, in order to provide thermal leads for the thermometers.

#### B. Measurements.

All measurements were performed in the tensile cryostat that has been previously described.<sup>(29)</sup> The brass end-pieces of the specimen were soft soldered into the mechanical grips which also serve as heat sinks. Two helium gas thermometer bulbs were soldered to the thermal leads. The thermometer system also has been described already. If an electrical current  $I$  passes through the sample, a voltage drop  $U$  arises between the thermometer bulbs. Since the thermometer tubing and the sample itself are electrically insulated,  $I$  and  $U$  can be measured. This is done by means of a six-stage Diesselhorst potentiometer. Because Joule heat is dissipated in the specimen, a temperature difference  $\Delta T$  is set up between the thermometers. The thermal conductivity  $\kappa$  is then given by

$$\kappa = \frac{1}{2} UI (d/F) \Delta T^{-1}, \quad (1)$$

where  $d$  and  $F$  are the distance between the thermometers and

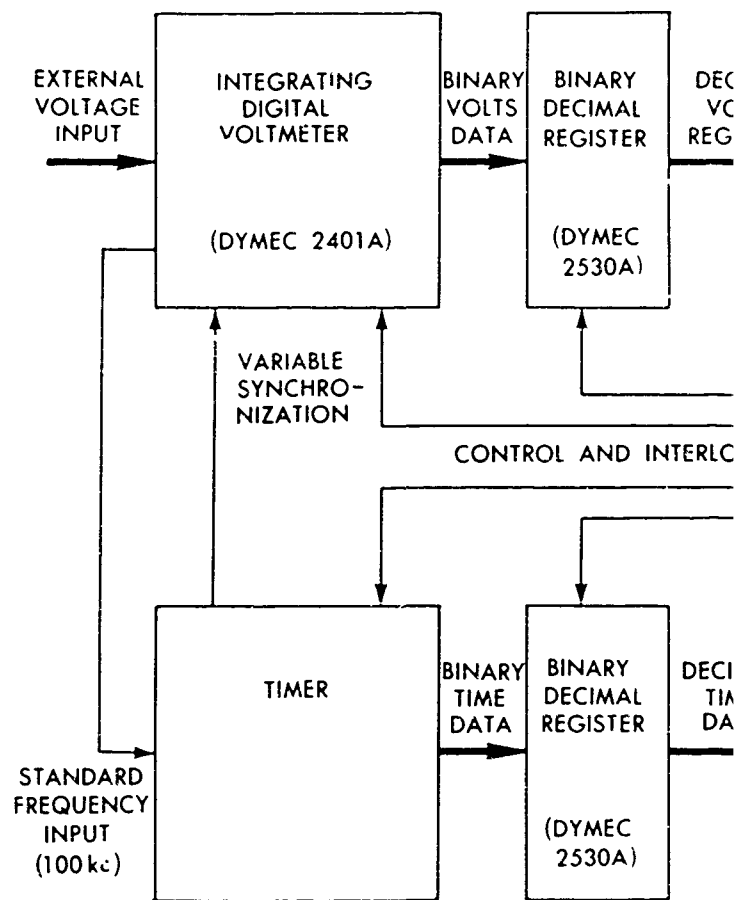
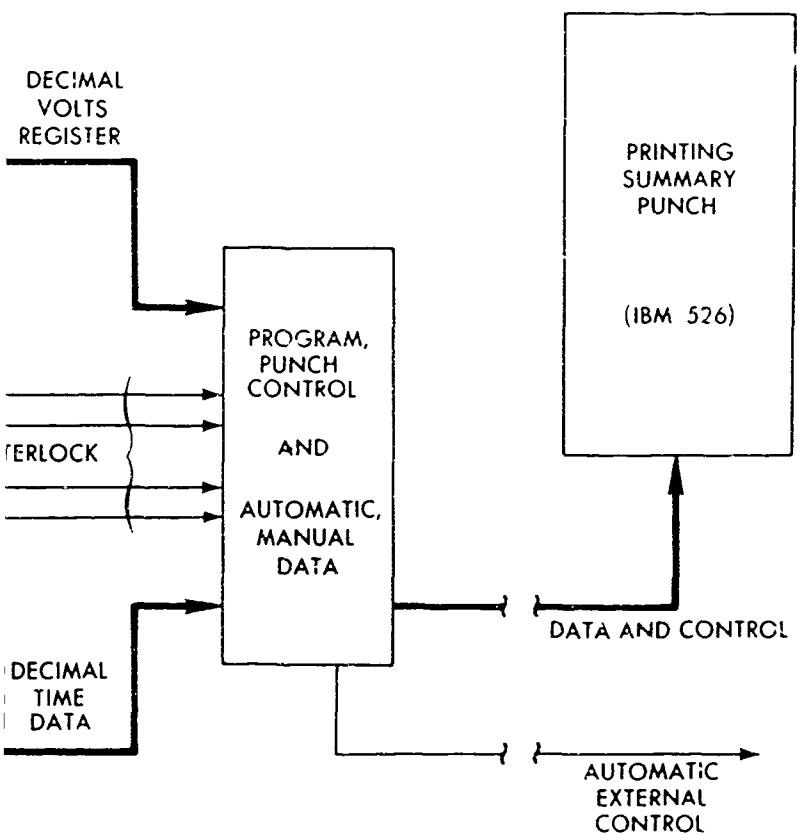


Fig. 2. Automatic digital data acquisition system. Data of the differential temperature and time of thermal transition are recorded on IBM cards.



data acquisition system.  
 differential temperature  $\Delta T$  (see Eq. 1)  
 cards, permitting machine evaluation  
 of transients. (29)

the sample cross-section, respectively. The electrical conductivity is

$$\lambda = (d/F) \cdot I/U . \quad (2)$$

For the specimens investigated in this work  $d/F$  had a value of 230 to 260  $\text{cm}^{-1}$ . The current was of the order 20 to 150 ma, and  $\Delta T$  did not exceed  $0.04^\circ\text{K}$  at an ambient temperature of  $4.2^\circ\text{K}$ . The relative accuracy in the measurements of  $\Delta T$  was of the order 0.1%.  $U$  and  $I$  were absolutely accurate by 0.1%,  $d/F$  by 0.8%. The main absolute error of  $\lambda$  was induced by errors in the calibration of the differential thermometer which are estimated to amount to approximately 5% or less.

The pressure inside the gas thermometers was measured by electrical transducers. The arising voltage was fed into a digital data acquisition system shown in Fig. 2. A 2-channel Speedomax recorder permitted us to optically follow the development of thermal transients, drifts, and the mechanical load on the specimen during the experiments.

### III. Results and Discussion

Fig. 3 shows the measured total thermal conductivity and the electrical conductivity of the Cu-Ni alloy system at  $4.2^\circ\text{K}$  for annealed specimens. The electrical resistance at this temperature is entirely due to solution disorder, and the validity of the Wiedemann-Franz law can be safely assumed. The separation

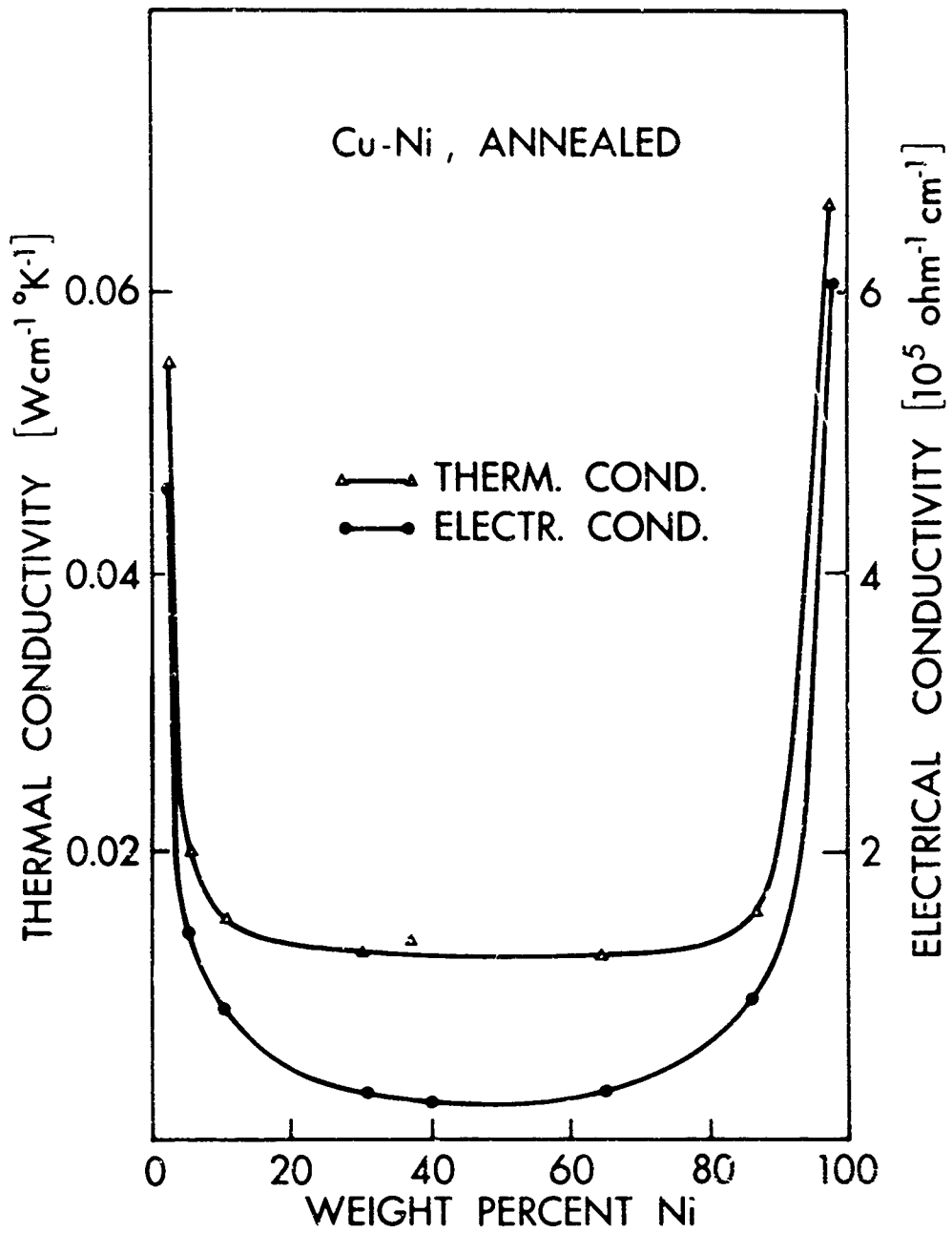


Fig. 3. Thermal and electrical conductivity at  $4.2^{\circ}\text{K}$  of annealed Cu-Ni alloy specimens.

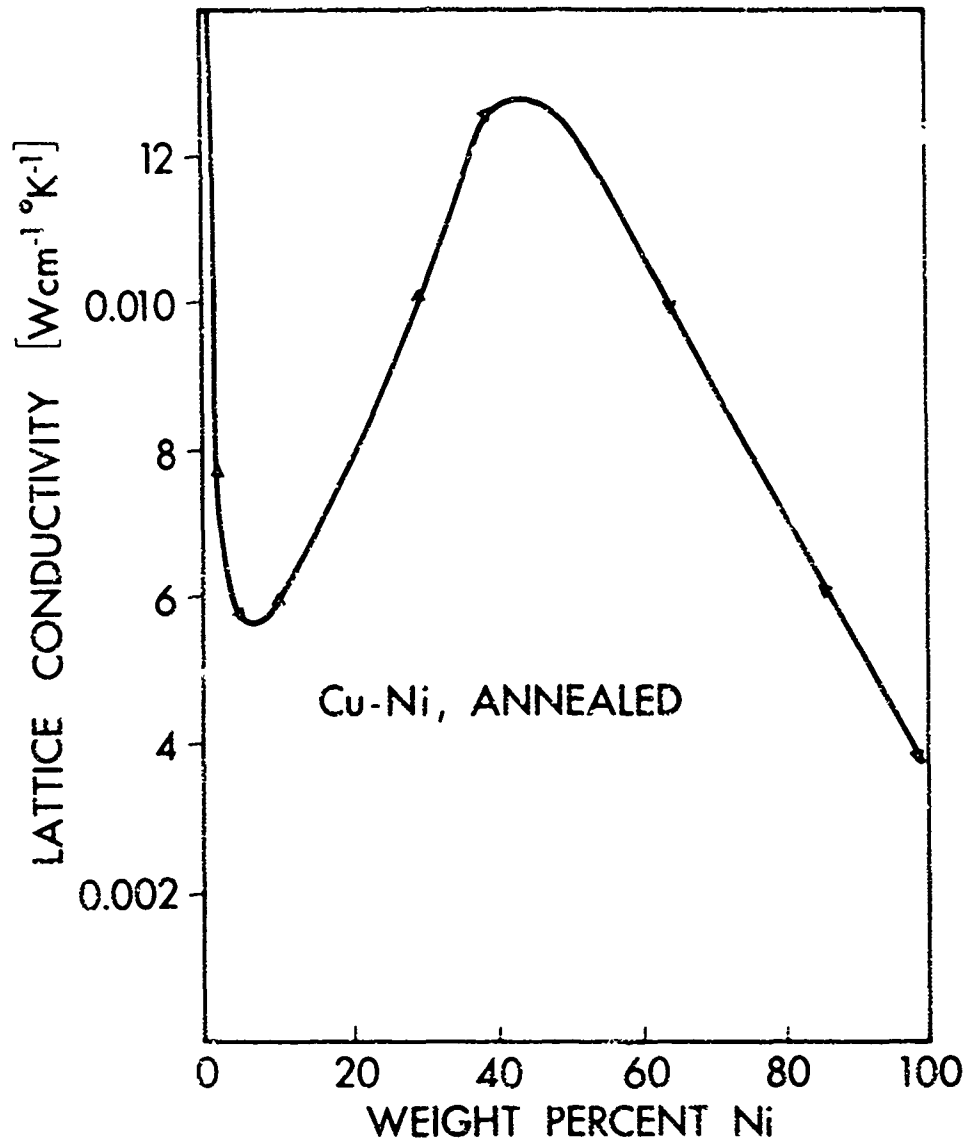


Fig. 4. Lattice thermal conductivity at 4.2°K of annealed Cu-Ni alloy specimens.

of the electronic and the lattice part of the total thermal conductivity can then be obtained from the relations

$$\begin{aligned}\kappa_e &= L T \lambda && \text{(electronic part)} \\ \kappa_g &= \kappa - \kappa_e && \text{(lattice part) ,}\end{aligned}\tag{3}$$

where  $L$  is the Wiedemann-Franz number with the value  $2.45 \cdot 10^{-8} \text{ W ohms } ^\circ\text{K}^{-2}$ .

The values of the lattice conductivity of the investigated alloys are plotted in Fig. 4. The value for pure copper has been determined by Klemens and amounts to approximately  $0.025 \text{ W cm}^{-1} \text{ } ^\circ\text{K}^{-1}$  at  $4.2^\circ\text{K}$ . The value of  $\kappa_g$  for pure nickel is not known.

The decrease of the lattice conductivity in Fig. 4 with increasing content of solute in the copper rich alloys, has often been found and has been discussed by Klemens, Tainsh and White.<sup>(21), (22)</sup> It is assumed that the scattering of electrons by the thermal motion of impurity ions, as it has been discussed by Koshino,<sup>(27)</sup> enhances the lattice resistance of metals containing small amounts of solute atoms. The thermal motion of the solute atoms adds an extra inelastic scattering contribution that is proportional to the impurity content.

On the nickel rich side of the diagram in Fig. 4, we do not observe a decrease of the lattice conductivity with solute

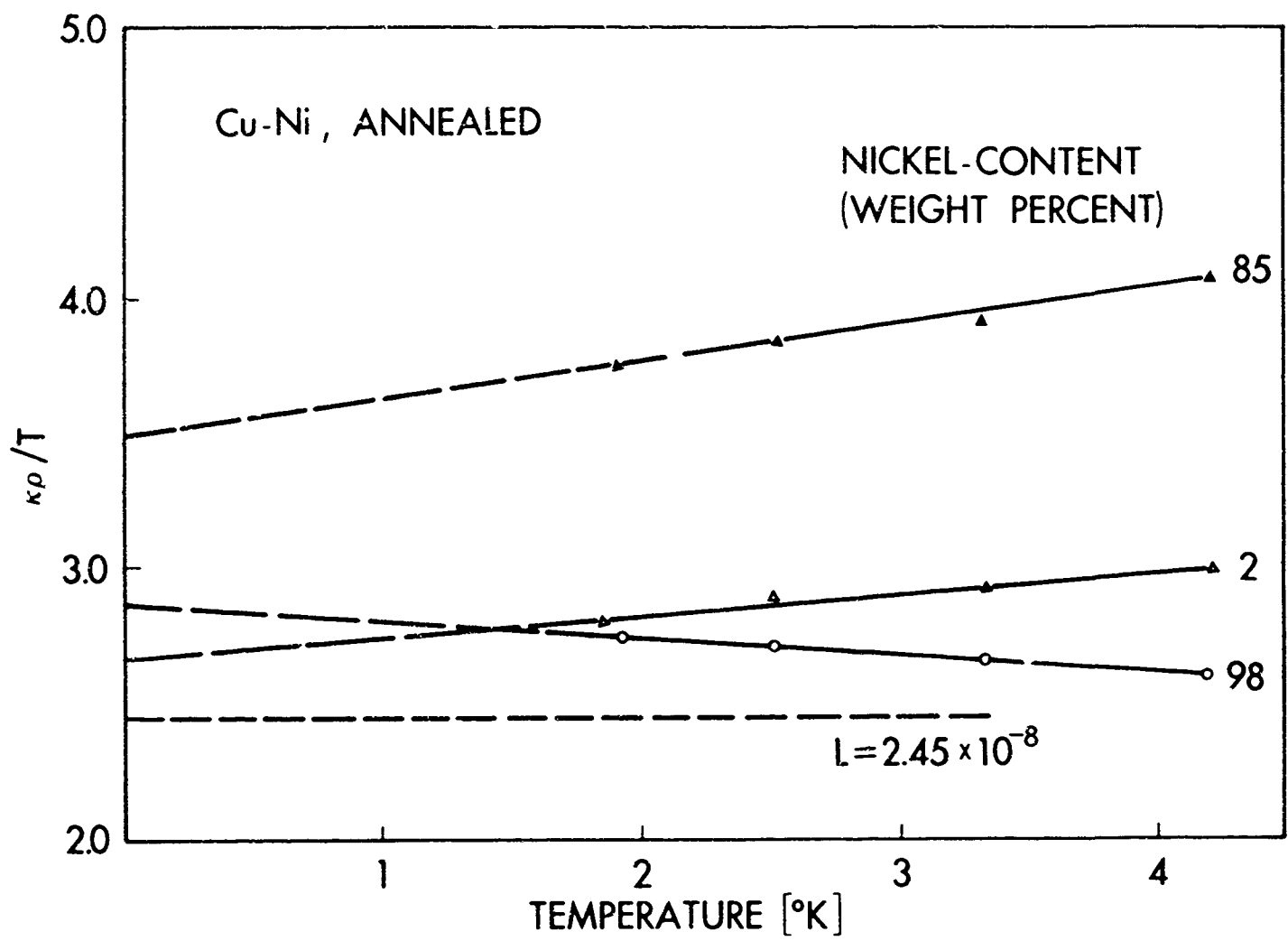


Fig. 5. Characteristic temperature dependence of three Cu-Ni alloys at helium temperatures. The alloy containing 98 weight percent nickel leads to a curve with a negative slope. See text.

content. Either we have to go to very dilute alloys on the nickel-rich side in order to detect the effect or, more likely, the effect is negligibly small in nickel containing small amounts of copper. It should be noticed that the lattice conductivity of the most nickel-rich alloy in Fig. 4 is only half the value of the corresponding copper-rich alloy on the left side of the diagram. The scattering process that limits  $\kappa_g$  on the nickel-rich side seems to be not merely scattering of phonons by electrons. In order to check this possibility, we have performed a few measurements of the temperature dependence of the total thermal conductivity in the helium range. If scattering of phonons by electrons is the dominant process limiting  $\kappa_g$ , the lattice conductivity should be proportional to  $T^2$ . If we then plot  $\kappa/T$  vs.  $T$ , we should obtain a straight line with a positive slope, since, according to Eq. (3),

$$\kappa/T = L\lambda + BT, \quad (4)$$

where  $L$ ,  $\lambda$ , and  $B$  are temperature independent.

In Fig. 5 plots of  $\kappa_p/T$  vs.  $T$  are shown for the alloys 868, 70, and 131, containing 2, 85 and 98 percent nickel, respectively. The plots for the alloys 868 and 70 have a positive slope. For alloy 131 however, a negative slope is obtained. Obviously Eq. (4) has to be modified in order to include an extra scattering process only important for the nickel-rich alloys.

Since nickel is a transition metal and ferromagnetic, we may expect additional scattering of phonons by spin-disorder. No theoretical work seems to be available on this subject. Bäcklund<sup>(30)</sup> has found similar indications in his work on iron alloys, however, in a higher temperature range.

Thus, certain anomalies occur on the nickel-rich side of the  $\kappa_g$  - composition diagram, which cannot be explained at present, but which may also bury the "Koshino-effect".

None of the plots in Fig. 5 follows Eq. (4) exactly. Otherwise, all curves would go through the point  $\kappa\rho/T = 2.34 \cdot 10^{-8}$  for  $T = 0$ . The deviations, which are smallest for the sample containing only 2 percent copper, are of the type observed originally by Zimmerman. The effect has been predicted by Pippard and occurs when the product of the electron mean free path  $\Lambda_e$  and the predominant phonon wave number  $q$  becomes smaller than unity, that is for an alloy with high electrical resistance. In that case the adiabatic approximation fails to be valid, since no proper interference conditions between phonons and electrons are established.<sup>(31)</sup> As a result, the lattice thermal resistance is smaller than it should be if there were enough interaction possible. Pippard's theory has been used by Zimmerman<sup>(25)</sup> and Lindenfeld and Pennsbaker<sup>(26)</sup> to explain the observed anomalies of the lattice conductivity in high-resistive alloys. It was found that in addition to the quadratic temperature term in the lattice conductivity a new term arises proportional to the temperature and

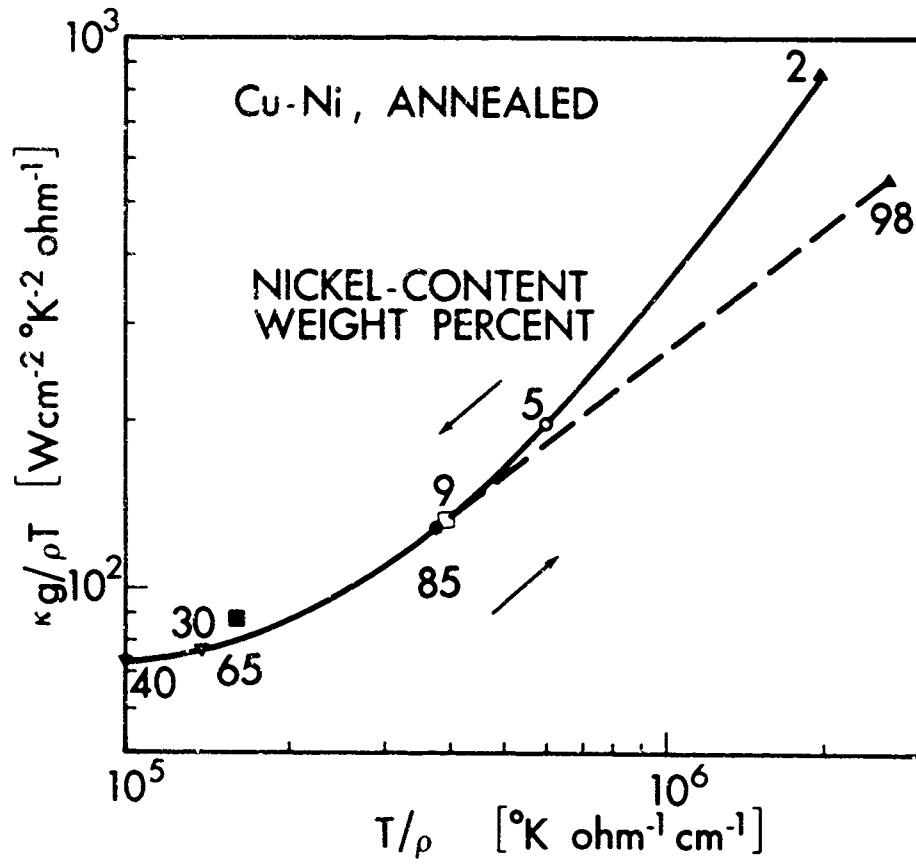


Fig. 6. The data of Fig. 4 replotted as  $\kappa_g/\rho T$  vs.  $T/\rho$ .

the electrical resistivity. In fact, the results for  $\kappa_g$  shown in Fig. 4, obtained for a constant temperature  $T = 4.2^\circ\text{K}$ , show the proportionality of  $\kappa_g$  and  $\rho$  over a large range of composition. The breakdown of the interference condition  $\rho\Lambda_e > 1$ , leading to an increase in the lattice conductivity, opposes the opposite effect of the inelastic impurity scattering on the left side of the diagram, leading to a minimum of  $\kappa_g$ . Similar effects showing an increase of  $\kappa_g$  with increasing solute content, after an initial decrease, have been found by Lindenfeld and Pennebaker in copper alloys containing a few percent germanium at temperatures around  $2^\circ\text{K}$ .<sup>(26)</sup>

The lattice conductivity for arbitrary values of  $\rho\Lambda_e$  has been calculated by Zimmerman<sup>(25)</sup> and Lindenfeld and Pennebaker.<sup>(26)</sup> The results can be compared with experimental values, if the observed ratio  $\kappa_g/\rho T$  is plotted vs.  $T/\rho$ . A universal curve has been obtained by the investigators in the comparison of their theory with experiments performed with high-resistive, but rather dilute silver and copper alloys. In Fig. 6 it is shown that even in the present case, where we are dealing with a complete system of binary alloys, most of the measured values of  $\kappa_g/\rho T$  fall on a smooth curve. Fig. 6 was obtained using the  $\kappa_g$  - values of Fig. 4, the  $\rho$  - values of Table I and putting  $T$  equal to  $4.23^\circ\text{K}$ .

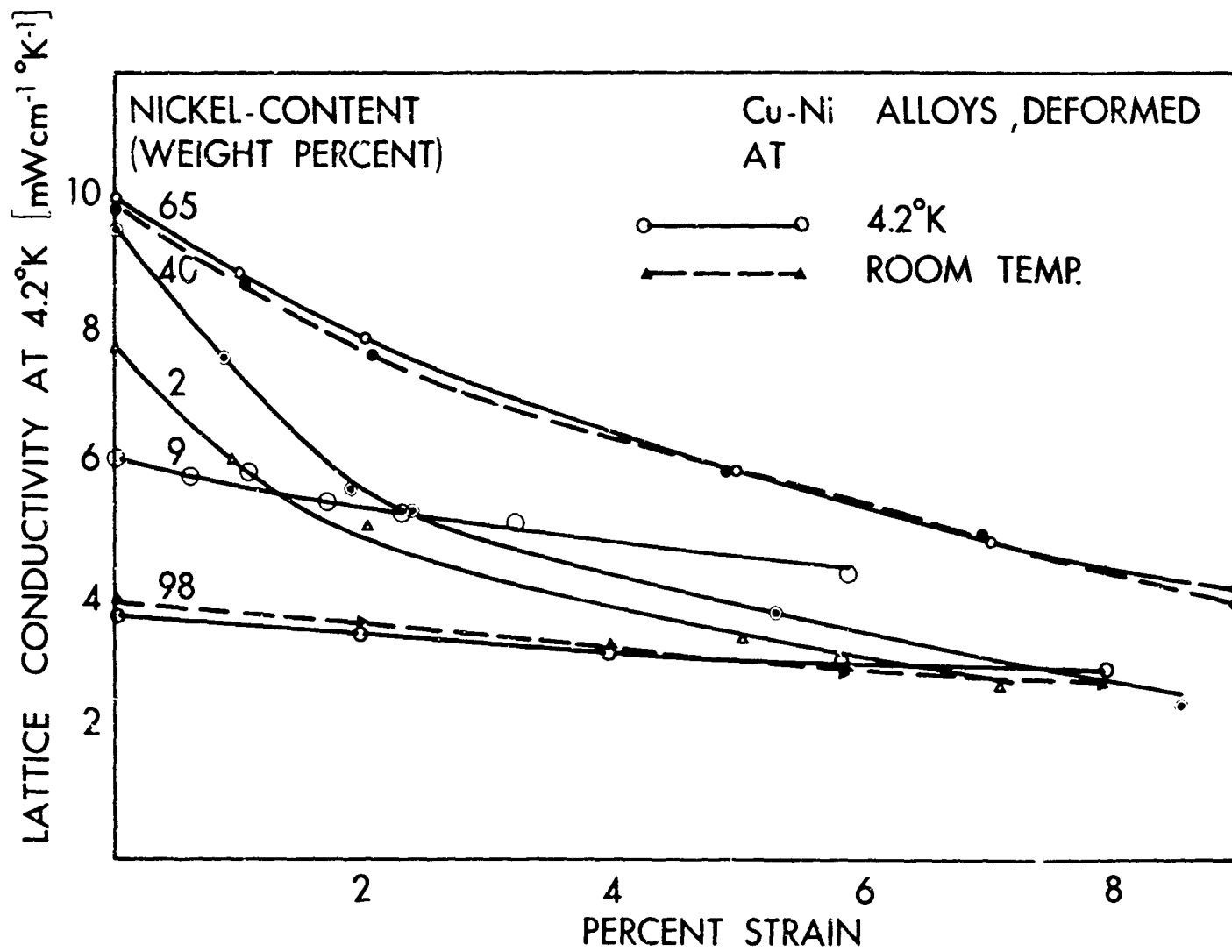


Fig. 7. The effect of plastic strain, applied at 4.2°K or 295°K, on the lattice thermal conductivity at 4.2°K of previously annealed Cu-Ni alloy specimens.

The point in Fig. 6 obtained for the most nickel-rich alloy 131 does not fall on the curve that connects all other points. This deviation is caused by two reasons: First, the variables of Fig. 6 actually have to be further reduced in order to account for the variation of the average sound velocity with the composition. The adjustment can be achieved approximately, if  $T$  is reduced to  $T/\theta$ , where  $\theta$  is the Debye characteristic temperature. If we chose  $\theta_{Cu} = 339$ ,  $\theta_{Ni} = 456^{\circ}K$ , the points for the two most dilute alloys, where this procedure may be permissible, fall closer together than in Fig. 6.

The second reason for the observed deviation of alloy 131 in Fig. 6 is suggested by the discrepancies already discussed in connection with Fig. 5. Scattering processes in addition to electron scattering might help to lower the lattice conductivity in the most nickel-rich alloys, arising perhaps from spin-disorder.

If plastic deformation is applied, the lattice conductivity is reduced considerably even for small strains. Fig. 7 shows some experimental results, which also show that room temperature deformation and deformation at  $4.2^{\circ}K$  have about the same effect. The reduction of  $\kappa_g$  is due to the scattering of phonons by dislocations, investigated theoretically by Klemens<sup>(3)-(7)</sup> and Bross et al.<sup>(9)-(11)</sup> Although in some instances good agreement between theory and experiment was found,<sup>(16)</sup> there is certainly a tendency in the available theories to underestimate the thermal resistance of a dislocation. As a consequence, dislocation densities

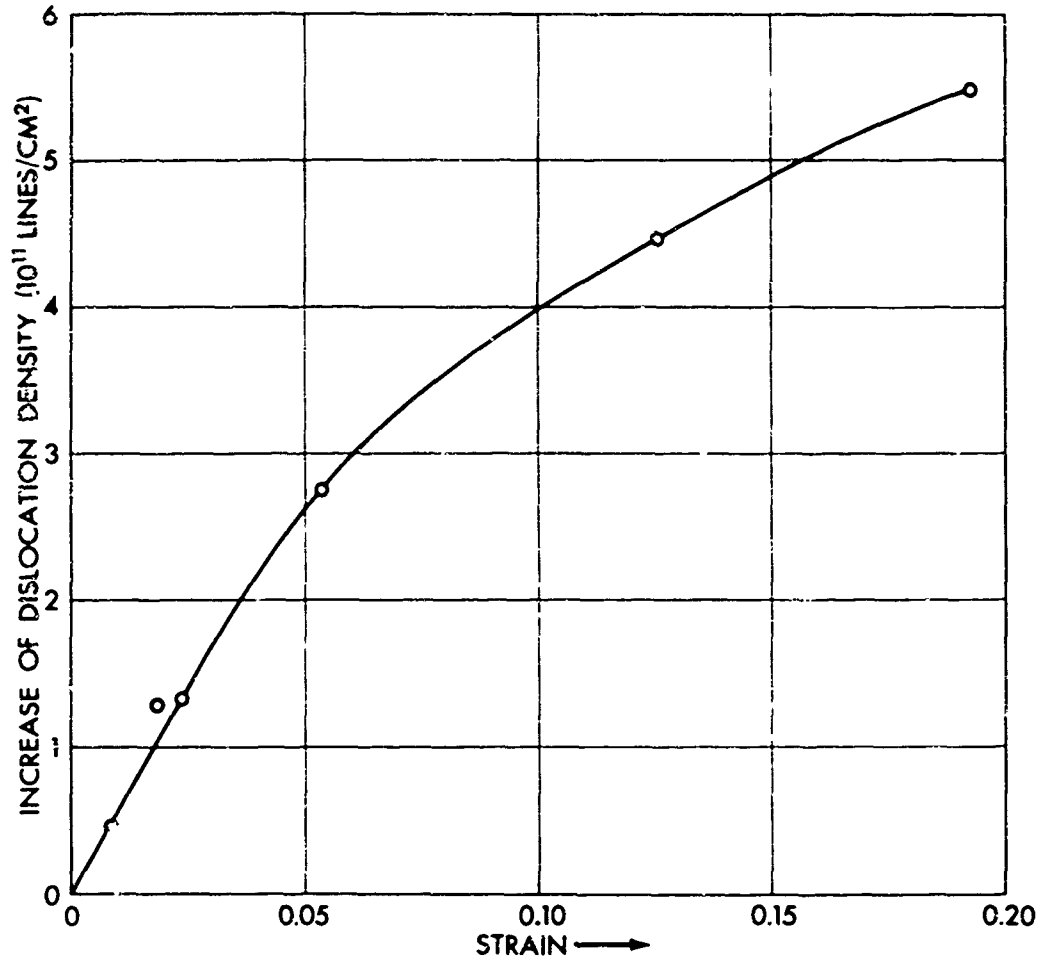


Fig. 8. Dislocation density of a Cu 60 - Ni 40 alloy specimen (K<sub>0</sub> in Table I), deformed at 4.2°K, as derived from measurements of the thermal conductivity. See text.

derived from experiments according to the current theories, have higher values than plausible. One example is shown in Fig. 8, where we have evaluated the dislocation density of a Cu 60 Ni 40 alloy after deformation at 4.2°K, using the theory of Klemens, which relates the additional lattice resistance  $W_D$  to the dislocation density  $N$  by

$$W_D = 0.17 (v h^2 / k^3) N b^2 \cdot T^{-2}, \quad (5)$$

where  $v$  is the phonon velocity,  $h$  Planck's constant,  $k$  Boltzmann's constant and  $b$  the Burgers vector. For copper,  $v = 2.27 \cdot 10^5$  cm/s,  $b^2 = 6.6 \cdot 10^{-16}$  cm<sup>2</sup>, for nickel  $v = 3.00 \cdot 10^5$  cm/s,  $b^2 = 6.2 \cdot 10^{-16}$  cm<sup>2</sup>. For Cu 60 - Ni 40 we thus obtain

$$W_D = 5.5 \cdot 10^{-9} N T^{-2} (\text{cm}^0 \text{K} \text{W}^{-1}). \quad (5a)$$

Bross et al have remarked that part of the discrepancy between the derived dislocation density as in Fig. 8 and the actual densities, which may be an order of magnitude lower, can perhaps be explained by the fact that actual dislocation patterns are piles rather than random distributions. Piles of dislocations have a stronger scattering power for phonons than an equal number of randomly distributed dislocations. All theories, however, have been based thus far on the assumption of random distribution and orientation.

Thus, we cannot place much significance on the obtained

values of the dislocation density. However, it seems that relative changes during deformation can be followed. In particular, Fig. 7 suggests that dislocation arrangements obtained after room temperature deformation and after deformation at 4,2°K cannot be very different in the case of the investigated alloys.

#### ACKNOWLEDGEMENTS

We wish to thank the International Nickel Company Inc., Research Laboratory, Bayonne, New Jersey for providing copper-nickel alloys together with their analysis. We also gratefully acknowledge the active help of Dr. R. M. N. Pelloux, Mrs. A. Raisanen and Miss Ursula Stark, who performed the micrographic analysis.

References

- (1) A. Sommerfeld and H. Bethe, in *Handbuch der Physik* (Springer-Verlag, Berlin, 1934), 2nd edition, Vol. 24/2, p. 545.
- (2) R. E. B. Makinson, *Proc. Camb. Phil. Soc.* 34, 474 (1938).
- (3) P. G. Klemens, *Proc. Roy. Soc. (London)* A208, 108 (1951).
- (4) G. Leibfried, in *Handbuch der Physik*, edited by S. Flügge (Springer-Verlag, Berlin, 1955), Vol. 7, Part 1, p. 290.
- (5) P. G. Klemens, *Proc. Phys. Soc. (London)* A68, 1113 (1955).
- (6) P. G. Klemens, in *Handbuch der Physik*, edited by S. Flügge (Springer-Verlag, Berlin, 1956), Vol. 14, p. 198.
- (7) P. G. Klemens, in *Solid State Physics*, edited by F. Seitz and D. Turnbull (Academic Press Inc., New York, 1958), Vol. 7, p.1.
- (8) J. Callaway, *Phys. Rev.* 113, 1046 (1959).
- (9) H. Bross, *Phys. Stat. Sol.* 2, 481 (1962).
- (10) H. Bross, A. Seeger, and R. Haberkorn, *Phys. Stat. Sol.* 3, 1126 (1963).
- (11) H. Bross, A. Seeger, and P. Gruner, *Ann. Phys. (Leipzig)* 7/11, 230 (1963).
- (12) R. E. Nettleton, *Phys. Rev.* 132, 2032 (1963).
- (13) K. R. Wilkinson and J. Wilks, *J. Sci. Instr.* 26, 19 (1949).
- (14) J. K. Hulon, *Proc. Phys. Soc. (London)* 64, 207 (1951).
- (15) I. Estermann and J. E. Zimmerman, *J. Appl. Phys.* 23, 578 (1952).

- (16) J. N. Lomer and H. M. Rosenberg, *Phil. Mag.* 4, 467 (1959).
- (17) W. R. G. Kemp, P. G. Klemens, and R. J. Tainsh, *Phil. Mag.* 4, 845 (1959).
- (18) W. R. G. Kemp and P. G. Klemens, *Austr. J. Phys.* 13, 247 (1960).
- (19) R. J. Tainsh, G. K. White, and P. G. Klemens, *Acta. Met.* 9, 966 (1961).
- (20) T. Olsen, *J. Phys. Chem. Solids* 12, 167 (1959).
- (21) R. J. Tainsh and G. K. White, *J. Phys. Chem. Solids* 23, 1329 (1962).
- (22) P. G. Klemens, G. K. White, and R. J. Tainsh *Phil. Mag.* 7, 1323 (1962).
- (23) D. Probert, *Nature* 201, 283 (1964).
- (24) M. S. R. Chari, *Proc. Phys. Soc.* 79, 1216 (1962).
- (25) J. E. Zimmermar, *J. Phys. Chem. Solids* 11, 299 (1959).
- (26) P. Lindenfeld and W. B. Pennebaker, *Phys. Rev.* 127, 1881 (1960).
- (27) S. Koshino, *Progr. Theor. Phys.* 24, 484 (1960).
- (28) A. B. Pippard, *J. Phys. Chem. Solids* 3, 175 (1957).
- (29) J. C. Erdmann and J. A. Jahoda, *Rev. Sci. Instr.* 34, 172 (1963).
- (30) N. G. Backlund, *J. Phys. Chem. Solids* 20, 1 (1961).
- (31) J. M. Ziman, *Electrons and Phonons* ( Clarendon Press, Oxford, 1960) p. 212.